EDMX Research Day 2025

4th February 2025, 11:00 – 18:00, Forum Rolex Centre

Time	Session	Speaker – Presentation – Activity
10:30 – 11:00	**Registration and coffee**	Mounting of posters on pinboards in Forum Rolex Centre
11:00 – 11:20	**Welcome & Introduction**	**Prof. Esther Amstad** EDMX Program Director
11:20 - 11:40	**Talk**	How curiosity brought the cat: From EPFL to CSEM, and a few steps in between **Dr. Eleonore Poli**
11:40 – 12:00	**Pitch talks*** Chair: Anja Tiede	1-minute talks by poster presenters (Public voting for prize)
12:00 – 13:15	**Lunch break & Poster session 1**	Odd numbers
13:15 – 14:15	**Doctoral students talks** Chair: Eva Baur	**Thanh Thi Hà Lê (LP) -** Glyoxylic Acid (GA)-Lignin as Paper Barrier Coatings for Food Packaging Applications **Raphaël Lemerle (LMSC) -** Selective area epitaxy to enhance the performance of Zn3P2/InP heterojunction solar cells **Sándor Lipscei (LMM) -** Oxide inclusions in steel: curse or blessing? **Torne Tänzer (CAM-X) -** 2D and 3D Small-angle X-ray Scattering of Human Lamellar Bone
14:15 – 15:30	**Coffee break & Poster session 2**	Even numbers
15:30 – 16:30	**Round table discussion** Chair: William Le Bas	**Introduction by EPFL Alumni Network** **Dr Amélie Bazzoni** **Dr Yves Condé** **Dr Maya Harris** **Dr Matteo Hirsch**
16:30 – 17:00	**Prize awards & Conclusions**	**Prof. Esther Amstad** EDMX Program Director
17:00 – 18:00	**Closing apéro**	

Scientific Committee: Dr Nuño Amador Mendez (LMSC), Dr Allison Chau (SMaL), Dr Sanggyu Chong (COSMO), Dr Antonia Georgopoulou (SMaL), Dr Julie Gheysen (LMM), Dr Deepika Sardana (SUNMIL), Dr Giannis Savva (THEOS), Dr Dagmara Trojanowska (LP)

Posters list (Posters marked with a * are giving pitch presentations)

Number	Name	Poster Title
1	Atreyee Acharya	Multiscale characterization of failed bioprosthetic heart valves using X-rays
2	Ilyana Ahmed-Khedda	Overcoming challenges in the implementation of low-carbon concrete
3	Zohreh Akbari	Effect of Ru Particle Size and Metal-Support Interactions on the Catalytic Hydrogen Combustion Performance
4	Disha Bandyopadhyay	Investigating self healing behaviour in physically crosslinked gels
5	Eva Baur	Microstructured elastomer and their macroscopic properties
6	Dhanush Sahasra Bejjarapu	Characterizing Chloride Resistance of Sustainable Cement Blends
7	Calixe Bénier	Tribology of ionic liquids
8	Francesca Bono	Enzymatic Mineralization of 3D Printable Granular Hydrogels
9	Nianduo Cai	Low-noise solid-state nanopore for improved resolution in biosensing
10	Nicola Carrara	Rhizosphere-sensitive nanoparticles
11	Mario Caserta	A dynamical Hubbard approach to the Mott-Hubbard/charge transfer series of transition-metal monoxides
12*	Ray Cowen	Understanding the Hydration Reaction and Surface Structure of Cementitious Calcium Silicate Hydrate via Solid-State NMR
13*	Matteo Darra	Mycelium-Nanocellulose hybrid materials
14	Blanca de Miguel Martinez	Polysaccharide nanomaterials from fungal fermentation
15	Axel Deenen	Non-equilibrium states in 3D superconducting nanoarchitectures
16	Gaëtan Denis	Electro-Sinter Forging of Ti/TiC composites
17	Enrico Di Lucente	Thermal backflow and rectification from phonon hydrodynamics for next-generation heat management devices
18	Anna Duvakina	Optically induced magnons from a metallic nanodisk
19	Andrea Fedrigucci	Comprehensive screening of plasma-facing Materials for nuclear fusion
20	Laurin E. Fischer	Dynamical simulations of many-body quantum chaos on a quantum computer
21	Rocio Garcia Montero	3D bioprinting of Functional Organoids at Room Temperature
22	Natan Garrivier	Multimodal X-ray and Neutron Studies of 3D-Printed RAFM steel-Tungsten Assemblies for Next-Gen Nuclear Energy Applications

23	Samuel Gatti	Towards new classes of materials: Performance Limitations of Sidorenkite-typeNa3Fe(PO4)(CO3) as a Na-ion Battery Cathode
24	Huixin Guo	3D magnonics and spintronics realized through additive manufacturing of free-form ferromagnetic nanodevices
25	Carolina Gutierrez Bolanos	Multi-scale characterization of fibers and composites using Small and Wide-Angle X-ray Scattering techniques
26*	Kyle Haas	Unassisted Photoelectrochemical Water Splitting: Plasmon-Assisted Catalysis Using Earth-Abundant Materials
27	Kamila Hamulka	Strain rate dependence of slip vs. twinning in c-axis compression of α-titanium
28	Yuki Hayashi	Growing functional multilayers from mycelium
29	Anthony Hoogmartens	Recyclable and Reshapable Composites Through an Energy-Efficient Photo-Induced Polymerization Method
30*	How Wei Bin	Adaptive energy reference for machine-learning models of the electronic density of states
31	Fei Hu	Polar Poly(Acrylonitrile) Thin Film Generated by Surface-Initiated Polymerization
32	Mohammad Jafarpour	Impact of Cavity Parameters on Gravure Printing for Printed Electronics
33	Hendrik Jansen	Tailored Nanocrystalline Aluminium Grain Size in a Nanolaminated Architecture: New Horizons
34	Matthias Kellner	Chemical shielding prediction in organic solids
35	Ayush Khurana	Investigation of tribo-corrosion properties of hydrogen embrittled steel
36	Anna Koptelova	Toward Multilayer Protein-Based Materials: Study of Single Layers
37	Stella Laperrousaz	Ultrasoft electronic fibers via thermal drawing
38	Thanh Thi Ha Le	Glyoxylic Acid (GA)-Lignin as Paper Barrier Coatings for Food Packaging Applications
39	William Le Bas	Strategies for Porosity Reduction in Direct Liquid Metal Deposition of Aluminium Alloys
40	Biruktait Ayele Lemecho	Compact, Multifunctional Integrated Device for Mars In-situ Propellant Production
41	Raphael Lemerle	Selective area epitaxy to improve performances of Zn3P2/InP heterojunction solar cell
42	Sándor Lipcsei	Insights into the local mechanical properties of manganese - silicate inclusions
43	Guoyuan Liu	Delta-learning interatomic potential for bulk nickel oxide based on multi-reference methods
44	Maja Lopandic	Designing Tetra-PEG Hydrogels with a Rhodamine Mechanophore to Study Force Transduction
45*	Yameng Lou	The Effect of Symmetry and Flexibility of Ligands on Super-selective Multivalent Interactions

46	Lorenzo Lucherini	Direct laser writing of metallic microstructures within soft hydrogel substrates
47	Marian Lumongsod-Thompson	Mechanistic understanding on the dissolution of siderite scale
48*	Arslan Mazitov	More accuracy with less data: a universal model for advanced atomistic simulations
49	Yan Meng	Chalcogenide Glass Nanowire Array by Thermal Drawing for Strong Optical Resonance
50	Camilla Minzoni	Advancing Metallic Thin Films Technology: ALD of Copper
51	Ceren Mitmit	Semi-Transparent Wide-Bandgap ACIGS Solar Cells by Low Temperature Processes
52	Seyyed Ezzatollah Moosavi	Precipitation in high recycled content 6xxx Aluminum sheet: Experiments and Model
53*	Timur Mukhametkaliyev	Minimum clinker (C-S-H) threshold of low clinker cements and alternative binders
54	Yann Muller	Constructing multicomponent cluster expansions with machine-learning and chemical embedding
55	Emie-kim Ngo Tan	Flexible LNP for in vivo mRNA delivery
56	Chiara Ongaro	Evaporated inorganic perovskite solar cells
57	Melis Özkan	Unveiling the Potential of Small Molecule Heparin Glycomimetics in Neuroregenerative Therapeutics
58	Claire Paetsch	Modeling hydrogen-metal interactions from first-principles
59*	Nataliya Paulish	Automated prediction of Fermi surfaces and de Haas-van Alphen oscillation frequencies from first principles
60*	Lorenzo Piersante	Training and assessing machine-learning interatomic potentials for studying structural phase transitions
61	Aleksandr Poliukhin	Electron-phonon interactions beyond DFT
62	Ekaterina Poliukhina	Cryo-ET as a Direct Method to Measure Colloidal Protein-Protein Interactions
63	Ferdinand Posva	Curvature-induced spin-triplet correlations in S(NbTiN)/F(Ni)/S Josephson junctions
64	Pierpaolo Ranieri	Quantitative measurement of electric field by 4D-STEM
65	Hari Priya Ravindran	Unravelling the interaction of superplasticizers with Calcium Aluminosulfates
66	Ding Ren	Protein-Rich Lipoprotein Nanoparticles for Melanoma Detection and Biomarkers Discovery
67	Linnea Rensmo	Deconvolving the shape and orientation information from the 3D reciprocal space map in SASTT experiments
68	Hien Tran Thi	Studying inhibition mechanisms of broad-spectrum antivirals with designed stoichiometric formulas and chemistry
69	Shixuan Shan	Magnetism of Single Tb adatoms on MgO

70	Elizaveta Shcherbacheva	In-situ liquid-phase electron microscopy of oxygen-evolving oxide catalysts
71	Cécilia Siri	Protein-small molecules interactions to stabilize proteins
72*	Deepak Somani	Predicting solute-defect interaction energies in dilute alloys from first-principles
73	Jinwon Song	Thermally drawn stretchable optical fibers
74	Marija Stojkovic	Predicting the suitability of photocatalysts for water splitting using Koopmans spectral functionals: The case of TiO2 polymorphs
75	Robin M. Studer	Salt Hydrate-Based Hydrogel Composite Materials for Energy Storage Applications
76	Divya Suman	Differentiable and transferable quantum chemistry through machine-learned electronic Hamiltonians
77	Torne Tänzer	2D and 3D Small-angle X-ray Scattering of Human Lamellar Bone
78	Buse Tatli	Engineering cellulose surfaces for improved nanofibrillation and redispersion
79*	Tushar Thakur	High-throughput computational screening of fast Li-ion conductors for solid-state electrolytes
80	Sophia Thiele	Investigation of the Dynamics in Supramolecular Networks by Solid-State NMR Spectroscopy
81	Anja Tiede	Sustainable photovoltaic schemes with compound semiconductors using correlated-disordered patterns
82	Saltanat Toleukhanova	Tri-layer graphene as membrane and electrode for liquid-phase electron microscopy studies of CO2 electroreduction nanocatalysts
83	Miguel Torre	Ion migration in carbon-based perovskite solar cells
84	Sici Wang	Computational development of small angle x-ray scattering tensor tomography
85	Matthieu Wendling	Phase Behavior of an Oligopeptide-Modified Polymer and a Matching Additive
86	Robert Wojtaszczyk	Understanding the Contribution of Calcium Aluminate Phases in Low-Clinker Portland Cements
87	Junfeng Xiao	Understanding the microstructure evolutions in NiTi alloys
88*	Mustafa Yalcinkaya	Enhancing In-Vitro Methods to Predict In-Vivo Biocorrosion of Magnesium Implants
89	Tianyu Yuan	3D-Printable DNGH-Based Pressure Sensor with Tunable Mechanical and Electrical Properties
90	Austin Zadoks	Machine learning Hubbard U
91	Michele Zendrini	III-V nanostructures for integration of 2D transition metal dichalcogenides

Glyoxylic Acid (GA)-Lignin as Paper Barrier Coatings for Food Packaging Applications

Thanh T. H. Le

PI: Prof. Harm-Anton Klok – Polymers Laboratory (LP)

Abstract

In response to growing demand for eco-friendly packaging, paper has become an attractive alternative to traditional materials due to its renewable and biodegradable nature. Thus, advances in paper coatings are essential to meet food packaging requirements for safety and preservation.

In this study, lignin—a key wood component—was used as the primary material for paper coating. Paper, mainly composed of cellulose and hemicellulose, gains additional value through the use of plant-based lignin, resulting in a single-sourced product, highlighting the enhanced value in utilizing plant-based materials. This lignin was functionalized with glyoxylic acid (GA), a commercially developed product by Bloom Biorenewables Ltd. in collaboration with EPFL[1]. The aldehyde-assisted fractionation (AAF) process uses GA as a protective group, preserving lignin's hydroxyl functional groups and preventing carbon-carbon bond formation, while also introducing carboxylic acid groups, which serve as versatile handles for further modifications or thermoset material development. Here, the reactivity of the hydroxyl and carbolic acid functional groups of lignin towards epoxides is taken advantage of to coat paper, which enhaces hydrophobicity and oil resistance of the substrate. The addition of the bis-epoxide crosslinkers, poly(ethylene glycol) diglycidyl ether (PEGDE) or glycerol diglycidyl ether (GDE) [2], helps improve the surface coating of the paperboards with better impregnation into the porous paper samples as compared to the GA-lignin coating without these crosslinkers. The flawless coatings, observed by SEM analyses, are achieved by the double-layered coating method, whether using PEGDE or GDE crosslinkers. Additionally, it is demonstrated that these coatings significantly enhance the paperboards' barrier properties to both oil and water, with particularly outstanding oil resistance exhibited by the double-layered coated samples. Furthermore, the application of GA-lignin-based coatings leads to an increase in the tensile strength and elasticity of the paperboards.

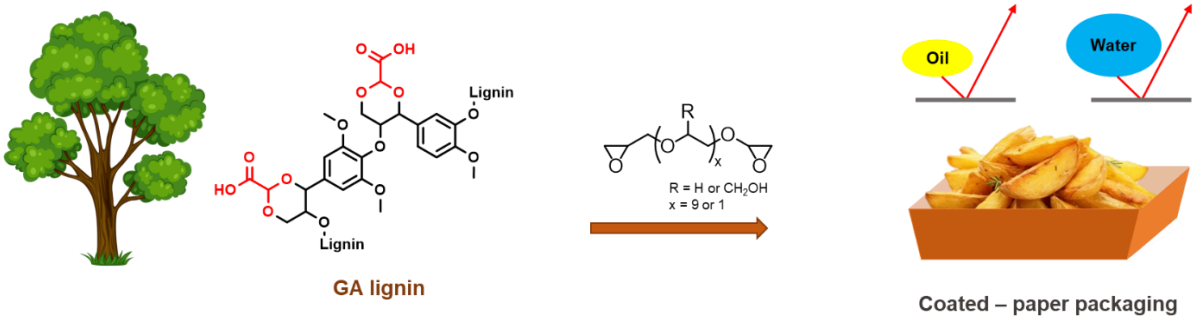

GA lignin

Coated – paper packaging

References

1. Bertella, S.; Bernardes Figueirêdo, M.; De Angelis, G.; Mourez, M.; Bourmaud, C.; Amstad, E.; Luterbacher, J. S., Extraction and Surfactant Properties of Glyoxylic Acid-Functionalized Lignin. *ChemSusChem* **2022,** *15* (15), e202200270.
2. Boarino, A.; Charmillot, J.; Figueirêdo, M. B.; Le, T. T.; Carrara, N.; Klok, H.-A., Ductile, High-Lignin-Content Thermoset Films and Coatings. *ACS Sustainable Chemistry & Engineering* **2023,** *11* (46), 16442–16452.

Selective area epitaxy to enhance the performance of Zn_3P_2/InP heterojunction solar cells

Raphaël Lemerle [a], Melanie Micali [b], Helena R. Freitas[c], Thomas Hagger [a], Didem Dede[a], Valerio Piazza [a], Maria Chiara Spadaro[c], Esther Alarcon Llado [b], Jordi Arbiol[c,d] and Anna Fontcuberta i Morral [a]

[a] Laboratory of Semiconductor Materials, Institute of Materials, School of Engineering, Ecole Polytechnique Fédérale de Lausanne, 1015, Lausanne, Switzerland
[b]Center for Nanophotonics, NWO-Institute AMOLF, Science Park 104, 1098 XG, Amsterdam, the Netherlands [c] Catalan Institute of Nanoscience and Nanotechnology (ICN2), CSIC and BIST, Campus UAB, Bellaterra, Barcelona, Catalonia, 08193, Spain.
[d]ICREA, Pg. Lluís Companys 23, 08010 Barcelona, Catalonia, Spain

Zinc phosphide (Zn_3P_2) is a promising material for low-cost photovoltaics made of earth-abundant elements. Its direct band gap of 1.5 eV makes it ideal for efficient photovoltaics. However, the record efficiency of 6% for a Zn_3P_2 solar cell achieved in the 1970s had never been outperformed ever since. The main obstacle was the synthesis of Zn_3P_2 with high crystal quality and controllable properties.

In this work, we explore selective area epitaxy (SAE) to improve the carrier transport by reducing the defect density. The idea is to grow the thin film starting from a nanoscale pattern enabling Zn_3P_2 pyramidal growth and subsequent merging. The films are grown on InP by Molecular Beam Epitaxy (MBE). Transmission Electron Microscopy (TEM) is used to characterize the microstructure of the films. Furthermore, we report on IV measurements on devices fabricated from SAE Zn_3P_2 thin films. Emphasis is placed on correlating the pattern dimensions with the device performances. Those results are supported by optical and electrical simulations. Finally, we demonstrate a Zn_3P_2 based solar cell with a conversion efficiency of 8.4%, setting a new record for the technology.

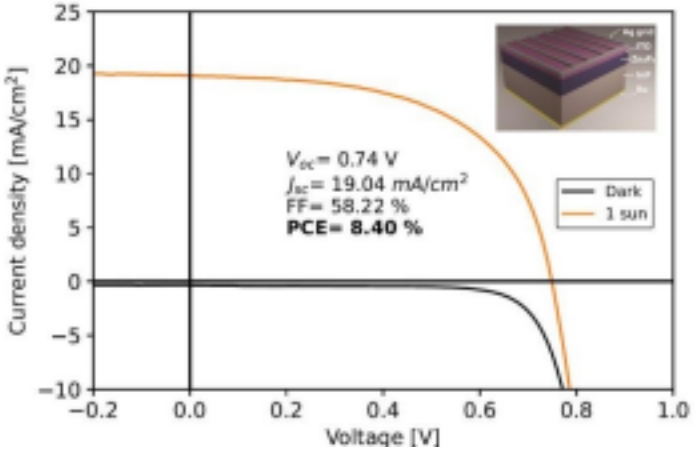

Figure 1: IV curve for a Zn_3P_2/InP heterojunction solar cell with record efficiency.

Oxide inclusions in steel: curse or blessing?

Sandor Lipcsei*[1],David Hernández-Escobar [1], Alejandra Slagter [1,2], and Andreas Mortensen[1]

[1] Laboratory of Mechanical Metallurgy, École Polytechnique Fédérale de Lausanne, Lausanne, 1015, Switzerland
[2] Present affiliation: Department of Materials Science and Engineering, Northwestern University, Evanston, Illinois, USA

*e-mail: sandor.lipcsei@epfl.ch

Keywords: inclusions, oxide, steel, nanoindentation, micromechanics;

In the previous century the steelmaking industry focused on the development of refining methods, aiming for the production of high purity alloys. In spite of tremendous efforts oxide inclusions remain unavoidable even in the highest quality steel. Additionally, steel contains a wide variety of inclusions, having a myriad of compositions and geometries. This recognition facilitated a shift towards the local physical and chemical adaptation of inclusions for the sake of minimizing their impact on the properties of steel. In order to fill an existing knowledge gap, the current project focuses on understanding the link between local chemical, microstructural and mechanical properties of oxide inclusions. To control the composition and microstructure of inclusions two methods are used, namely sequential arc melting methodology and skull melting, followed by optional heat treatments. The composition and crystallinity of inclusions are studied by scanning electron microscopy (SEM), transmission electron microscopy (TEM) and Raman spectroscopy. Inclusion hardness and elastic modulus are determined by nanoindentation, taking into account the inclusion – matrix elastic mismatch [1]. It was found that the degree of crystallinity strongly correlates with superior mechanical properties, having implications on the inclusion – matrix system fatigue properties. In the framework of in-situ micromechanical testing the strength of inclusions [2], as well as the inclusion – matrix interfacial strength are studied [3]. The tests have shown that silicon oxide inclusions can approach the strength of the corresponding theoretical limit [2], while iron - silica interfacial strength is in the order of gigapascals. On the other hand, manganese-silicates are just as strong, as the interface, having consequences on their deformability.

References:

[1] Slagter, A., Everaerts, J., & Mortensen, A. (2023). Nanoindentation of embedded particles. *Journal of Materials Research*, *38*(6), 1694-1705.

[2] Slagter, A., Everaerts, J., Deillon, L., & Mortensen, A. (2023). Strong silicon oxide inclusions in iron. *Acta Materialia*, *242*, 118437.

[3] Hernández-Escobar, D., Slagter, A., Amarillo, S. P., & Mortensen, A. (2024). Room-temperature strength of the interfacial bond between silica inclusions and iron. *Acta Materialia*, *263*, 119502.

2D and 3D Small-angle X-ray Scattering of Human Lamellar Bone

Torne Tänzer[a,b], Tatiana Kochetkova[c], Mathieu Simon[c], Carolina Gutiérrez Bolaños[a,b], Mads Carlsen[a], Philippe Zysset[c], Marianne Liebi[a,b]

[a]Paul Scherrer Institut (PSI), Villigen, Switzerland
[b]Institut des Matériaux (IMX), Ecole Polytechnique Fédérale de Lausanne (EPFL), Switzerland [c]ARTORG Center for Biomedical Engineering Research, University of Bern, Switzerland

Despite the dominant role of bone mass in fragility fractures, the effect of microstructure on bone strength and fracture risk can not be neglected. In order to gain insight on bone's structure property relations, a clearer understanding of the hierarchical organization of the collagen fibres and mineral phase is required.

Using scanning small-angle X-ray scattering (sSAXS) in 2D and in 3D (SAXS tensor tomography) [1], this work aims to provide new insight into bone microstructure across multiple length scales. SASTT is an extension of synchrotron scanning SAXS, allowing for reconstruction of the scattering signal in a volume resolved manner in 3D macroscopic samples.

Bone micropillars were characterized by SASTT with three different beamsizes (25µm^2, 5µm^2 and 2µm^2), aiming to provide structural characterization at the levels of the whole tissue, single osteons and individual lamellae. Tissue-scale and osteon level measurements were respectively performed at the cSAXS and PX-I beamlines of the Swiss Light Source, and lamellar samples were measured at the ID13 beamline of the European Synchotron Radiation Facility (ESRF).

Recent developments in tensor tomographic reconstruction algorithms[2] have led to the possibility to characterize the 3D reciprocal space map (RSM) with much greater detail, such as extracting multiple orientations and symmetries.

Figure 1 illustrates the nanostructural differences on the smallest length scale studied, suggesting alternating ultrastructural organization of adjacent lamellae. In order to obtain structural characterization with statistical relevance, a 2D sSAXS beamtime was performed on a larger sample set, allowing for the comparison of structural parameters with anatomical location and donor age. This work demonstrates how the SASTT characterization of microstructural parameters over multiple length scales, complemented with 2D measurements on a larger dataset, contributes to unveiling a clearer understanding of bone microstructure.

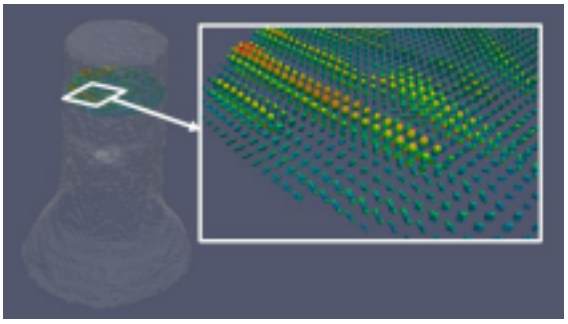

Figure 1: SASTT reconstruction of a lamellar bone pillar. In each voxel, the RSM of a specific scattering amplitude is represented by a sphere, deformed and colored proportionally to the intensity in each direction. A horizontal slice of RSMs is displayed, illustrating alternating lamellae of strong longitudinal scattering and weaker disordered scattering.

References:

[1] Liebi, M., Georgiadis, M., Menzel, A. *et al.*, *Nature* **527**, 349–352 (2015). [2] Nielsen, L., Erhart, P., Guizar-Sicairos, M. & Liebi, M., Acta Cryst. **A79**, 515-526 (2023).